CFSRC COLLOQUIUM

Proceedings of the Cold-Formed Steel Research Consortium Colloquium
17-19 October 2022 (cfsrc.org)

Sheathing Braced Design of CFS Wall Panels: Review and Proposal

Sivaganesh Selvaraj[1], Mahendrakumar Madhavan[2]

Abstract

The objective of this investigation is to understand the existing design rules of sheathed cold-formed steel (CFS) members. A comprehensive analytical study on the stiffnesses offered by the sheathing to the CFS panel was conducted. Three different combinations of stiffnesses that are offered by the sheathing were examined based on the failure modes and ultimate moment capacities obtained from the experimental results. The experimental results were compared with the predicted design strengths using the existing design approaches available. The deficiency of the current design approaches are highlighted, and a modified approach for incorporating the stiffnesses that are offered by the sheathing in the elastic buckling analysis is presented. The design strengths predicted using the modified approach on stiffness selection showed good agreement with the ultimate moments obtained from the experiments. A reliability analysis performed indicates that the modified design approach presented in this work can be employed for the design of gypsum sheathed cold-formed steel members subjected to bending (out-of-plane).

1. General

Sheathed CFS member design, especially two-sided, with an advantage of having an increased strength due to reduced slenderness compared to the unsheathed one is gaining interest in the construction industries as well as among researchers, which is the interest of the present study. CFS members subjected to various loading conditions behaves differently resulting in complex failure modes [1], and hence requires special attention while designing them. In the same vein, such special attention is equally important for sheathed CFS members. The design calculations for sheathed CFS wall panel subjected to axial compression and flexure is available in the recent AISI's research report RP13-1 titled "Sheathing Braced Design of Wall Studs" [2]. The AISI (2013a) [2] design method adopted the Direct Strength Method (DSM) of North American Specification for cold-formed steel structures [3] for the sheathed CFS panel design. The AISI (2013a) [2] has classified the effect of sheathing on CFS structural member into three different stiffness components for each sheathing fastener connections as shown in Fig. 1a. These three different stiffness components were derived from distinct experimental setups recommended by Winter [4-5] for restraint against lateral movement, AISI S901 [6] for restraint against cross section twist and ASTM E72-15 [7] for additional flexural rigidity for flexural bending. In addition, the AISI (2013a) [2] recommends the simultaneous application of the above-mentioned stiffnesses (all together) in design strength calculations of sheathed CFS panels for both axial compression and out of plane loading conditions.

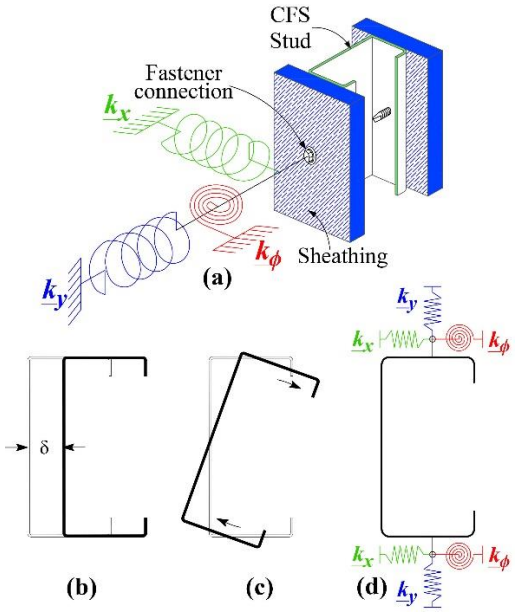

Fig. 1. Cold-Formed Steel Sheathed Structural Members - (a) Stiffness components at each Sheathing fastener connections; (b) Failure mode (Cross sectional view) - Weak axis buckling when subjected to axial compression; (c) Failure mode (Cross sectional view) - Lateral torsional buckling when subjected to flexure; (d) Incorporating sheathing stiffnesses in the elastic buckling analysis

[1] Postdoctoral fellow, Department of Civil and Environmental Engineering, The Hong Kong Polytechnic University, Hong Kong. sivaganesh.selvaraj@polyu.edu.hk
[2] Professor, Department of Civil Engineering, Indian Institute of Technology Hyderabad, Telangana, India. mkm@ce.iith.ac.in

The highly slender CFS member subjected to axial compression may fail due to weak axis buckling as shown in Fig. 1b [deflects laterally without twist or change in cross-sectional shape [3]]. However, when such highly slender members are attached to sheathing, then the attached sheathing offers resistance against the lateral movement by shear and bearing force that is generated at each sheathing-fastener connection in the CFS stud. However, the same unsheathed CFS member will undergo lateral-torsional buckling (LTB) as shown in Fig. 1c [out of plane bending occurring simultaneously with a twist about the shear center (AISI 2012a) [3]] in case of flexural loading. When such a member is attached to sheathing, the sheathing provides resistance to twist of the CFS member (movement of the two flanges in opposite side) by bearing. Hence, it appears that the components of stiffness offered by the attached sheathing are dependent on the loading conditions and failure mode of the CFS member. The investigation carried out in this paper is aimed to provide some preliminary suggestions on selecting the stiffness components for flexural strength determination of sheathed CFS panel by carrying out design calculations using different combinations of sheathing stiffnesses arrived according to AISI (2013a) [2]. The strength calculations are presented for each of the sheathing stiffness combinations arrived. The procedures to calculate the stiffness components of the sheathing fastener connection are presented. The different composite actions between the sheathing and CFS structural member are examined, and the appropriate one for calculating the design strength is suggested. The reliability analysis for sheathed CFS panel design was also carried out by comparing the design predictions with the experimental results obtained.

2. Sheathing braced design of CFS member using DSM

The proposed design method incorporated the bracing effect that arises at each fastener sheathing connections by carrying out an elastic buckling analysis which is an input to the DSM method of AISI (2012a) [3]. As discussed previously in the introduction section, the bracing effect was categorized into three different directional stiffnesses at each fastener sheathing connections as shown in Fig. 1a. Those stiffnesses are k_x (lateral translational stiffness), k_y (out of plane vertical translational stiffness) and k_ϕ (stiffness against the cross-sectional rotation of the CFS stud). The stiffnesses (k_x, k_y, *and* k_ϕ) at the fastener sheathing connections are calculated as a function of the mechanical properties of the sheathing material, screws/fasteners, and CFS stud. Although this design method (stiffness + DSM) was proposed for both the compression and out of plane loading cases by AISI (2013a) [2] the effectiveness of the design equations for various slenderness of the CFS stud is not yet verified for both axial and flexural loading cases as per the author's knowledge. Therefore, the present study concentrates on the increase in the design strength due to a change in the failure mode of two-sided gypsum sheathed CFS member subjected to out-of-plane bending. More information on experimental test setup for out-of-plane loading of sheathed CFS panel, specimen details, experimental failure modes and experimental moment values (M_{EXP}) are presented in Selvaraj and Madhavan [8].

The following are the Eqs. (1, 4 and 9) to determine the stiffnesses k_x, k_y, and k_ϕ. The mechanism behind the derivations of the following expressions are explained in Vieira and Schafer [9-10]. The Eq. (1) for determining the lateral translational stiffness combines two distinct mechanisms; (i) the local stiffness (k_{xl}) [Eq. (2)] developed at the fastener sheathing connection against the bearing and tilting of the fastener; (ii) the diaphragm stiffness (k_{xd}) [Eq. (3)] provided by the sheathing when the CFS structural members subjected to axial compression undergoes minor axis bending.

$$k_x = \frac{1}{\frac{1}{k_{xl}}+\frac{1}{k_{xd}}} \quad (1)$$

$$k_{xl} = \frac{3\pi E_s d^4 t^3}{4t_b^2(9\pi d^4+16t_b t^3)} \quad (2)$$

$$k_{xd} = \frac{\pi G_b t_b d_f w_{tf}}{L^2} \quad (3)$$

where E_s = Young's modulus of the CFS structural member measured by testing as per ASTM E8 (ASTM 2013) [11]; d = diameter of the fastener; t = thickness of the CFS structural member that is attached to the sheathing; t_b = thickness of the gypsum sheathing board; G_b = shear modulus of the sheathing that may be obtained from Table C4.2.2B of ANSI (2005) (Specification by American Forest and Paper Association (AF&PA) & American Wood Council (AWC)) [12]; d_f = intermediate fastener spacing; w_{tf} = tributary width of the panel to the fastener; L = c/c distance between the supports of the wall panel.

Equation (4) is the out of plane translational stiffness (k), acting in the direction of the strong axis, which may be considered in three different ways of composite action between the sheathing and the CFS structural member. Assuming (i) no composite action (k_y); (ii) partial composite action (k_{yp}) (should be arrived by conducting a bending test of the same panel); and (iii) full composite action (k_{yf}) (by adding the flexural stiffness of the sheathing board). If no composite action is considered then the Eq. (4) can be used directly which considers the flexural rigidity $(EI)_w$ of the sheathing board alone. For partial composite action, the sheathed wall panel should be tested under the strong axis bending as per ASTM-E72-15 [7] to find the true flexural rigidity of the sheathing board [$(EI)_{pc}$] [Eq.(6)]. After determining the full flexural stiffness of the wall panel by testing [$(EI)_{system}$] [Eq. (5)], the flexural stiffness of the CFS

structural member [$(EI)_{stud}$] should be subtracted, and only one half of the remaining stiffness should be considered if the panel is identically sheathed on both the sides as shown in Eq. (6). For full composite action between CFS structural member and sheathing board, which includes the inertia of the sheathing board, $(EI)_{fc}$ is calculated as described in Eq. 7.

$$k = \frac{(EI)_i\ \pi^4 d_f}{L^4} \tag{4}$$

$(EI)_i = (EI)_w$ *when no composite action is considered ($k=k_y$)*
$(EI)_i = (EI)_{pc}$ *when partial composite action is considered ($k=k_{yp}$)*
$(EI)_i = (EI)_{fc}$ *when full composite action is considered ($k=k_{yf}$)*

$$(EI)_{stud}\ (or)(EI)_{system} = \frac{11WL^3}{384\delta} \tag{5}$$

$$(EI)_{pc} = \frac{1}{2}\left[(EI)_{system} - (EI)_{stud}\right] \tag{6}$$

$$(EI)_{fc} = (EI)_w + E_w\, w_{tf}\, t_b(\frac{1}{2}h + \frac{1}{2}t_b)^2 \tag{7}$$

$$E_w = \frac{12\,(EI)_w}{w_{tf} t_b^3} \tag{8}$$

Where $(EI)_i$ is the flexural rigidity/stiffness of the sheathing board; $(EI)_w$ is the effective sheathing stiffness obtained from Table 2 of GA-235-10 [13] based on the orientation of the sheathing board; W is the load applied, and δ is the out of plane deflection to the respective load (W) from strong axis bending test of the sheathed wall panel as per ASTM-E72-15 [7]; h is the depth of the CFS stud (out-to-out), and E_w is the bending modulus of the sheathing material that is calculated from the effective sheathing stiffness $(EI)_w$ obtained from GA-235-10 [13] using Eq.8 . The $(EI)_{stud}$ may be calculated manually or obtained from the strong axis bending test results of unsheathed CFS structural member, the W and δ values of the unsheathed CFS studs may be replaced in the Eq.(5) to obtain the flexural rigidity of the stud [$(EI)_{stud}$]**.** In the present work, the $(EI)_{stud}$ was calculated manually by factoring the major axis moment of inertia of the CFS stud (I_{xx}) and Young's modulus (E_s) obtained from the coupon tests results presented in the companion paper. It should be noted in Table 1 that the calculated partial composite action stiffness (k_{yp}) values are higher than the full composite action stiffness (k_{yf}) due to the conservativeness of the Eqs. (7 and 8). In the present study, both the full composite (k_{yf}) and partial composite action (k_{yp}) stiffnesses were examined for each CFS studs.

The stiffness that resists the twisting of the cross-section of the CFS channel is rotational stiffness, k_ϕ. Similar to the lateral translational stiffness (k_x), the k_ϕ is having sheathing rotational restraint ($\underline{k}_{\phi w}$) and connection rotational stiffness ($\underline{k}_{\phi c}$) separately. The value of k_ϕ can be obtained from the following equations:

$$k_\phi = \underline{k}_\phi\ d_f \tag{9}$$

$$\underline{k}_\phi = \frac{1}{\underline{k}_{\phi w}} + \frac{1}{\underline{k}_{\phi c}} \tag{10}$$

$$\underline{k}_{\phi w} = \frac{2EI_w}{d_f} \tag{11}$$

$$\underline{k}_{\phi c} = 0.00035E_s t^2 + 75 \tag{12}$$

where E_s is Young's modulus of the CFS stud in units of pounds-force per square inch (lb-f/in^2), and t, a flange thickness of the CFS stud, is given in inches. The Eq. 12 for finding the connection rotational stiffness ($\underline{k}_{\phi c}$) was suggested by Schafer et al. [14]. In addition, it should also be noted that the value of connection rotational stiffness $\underline{k}_{\phi c}$ can also be obtained from the Table Z.1-2[1] of AISI [2] report. In comparison with the rotational restraint values obtained from Eq. (12) the values given in Table Z.1-2[1] of AISI [2] were upper bound. The appropriateness of the values of $\underline{k}_{\phi c}$ obtained from Eq. (12) and from Table Z.1-2[1] of AISI [2] is examined in the present study. Therefore, the k_ϕ values calculated using the $\underline{k}_{\phi c}$ values obtained from Table Z.1-2[1] of AISI [2] and Eq. (12) of AISI (2013a) [2] will be termed as "$\underline{k}_\phi$ (T)" and "$\underline{k}_\phi$ (Eq)" respectively.

3. DSM equations for flexural strength predictions

The DSM expressions for beam design from section 1.2.2 of AISI S100-12 (AISI 2012a) [3] are summarized below. The nominal flexural strength or unfactored design strength (M_{DSM}) is the minimum of the nominal flexural strengths for LTB strength (M_{ne}), local buckling (M_{nl}), and distortional buckling (M_{nd}), as shown in Eq. (13). In addition, AISI [3] allows to include the inelastic reserve buckling capacities of local and distortional buckling in the design as per the Eqs. (18 and 20) if the CFS member is adequately braced from LTB by sheathing or bridging.

$$M_{DSM} = \min(M_{ne}, M_{nl}\ and\ M_{nd}) \tag{13}$$

Lateral-torsional buckling strength (M_{ne})

$$M_{ne} = M_{cre} \quad \text{for } \mathrm{M}_{cre} < 0.56\,\mathrm{M}_y \tag{14}$$

$$M_{ne} = \frac{10}{9}M_y\left(1 - \frac{10M_y}{36M_{cre}}\right) \text{for } 2.78\,\mathrm{M}_y \geq \mathrm{M}_{cre} \geq 0.56\,\mathrm{M}_y \tag{15}$$

$$M_{ne} = \mathrm{M}_y \quad \text{for } \mathrm{M}_{cre} > 2.78\,\mathrm{M}_y \tag{16}$$

Local buckling strength (M_{nl})

$$M_{nl} = \mathrm{M}_{ne} \quad \text{for } \lambda_l \leq 0.776 \tag{17}$$

$$M_{nl} = M_y + \left(1 - \frac{1}{C_{yl}^2}\right)\left(M_p - M_y\right) \text{for } \lambda_l \leq 0.776 \text{ and } \mathrm{M}_{ne} \geq M_y \tag{18}$$

$$M_{nl} = \left[1 - 0.15\left(\frac{M_{crl}}{M_y}\right)^{0.4}\right]\left(\frac{M_{crl}}{M_y}\right)^{0.4} M_y \quad \text{for } \lambda_l > 0.776 \qquad (19)$$

Distortional buckling strength (M_{nd})

$$M_{nd} = M_y + \left(1 - \frac{1}{C_{yd}^2}\right)(M_p - M_y) \quad \text{for } \lambda_d \leq 0.673 \qquad (20)$$

$$M_{nd} = \left[1 - 0.22\left(\frac{M_{cd}}{M_y}\right)^{0.5}\right]\left(\frac{M_{crd}}{M_y}\right)^{0.5} M_y \quad \text{for } \lambda_d > 0.673 \qquad (21)$$

where M_{cre} = critical elastic lateral-torsional buckling moment; $M_{cre} = S_f\ f_{cre}$; M_y = member yield moment; $M_y = S_f\ f_y$; M_p = member plastic moment; $M_p = Z_f\ f_y$; S_f = gross section modulus (first yield); Z_f = plastic section modulus; f_y = yield stress obtained from tensile coupon tests; $C_{yl} = \sqrt{(0.776 / \lambda_l)} \leq 3$; $\lambda_l = \sqrt{(M_y / M_{crl})}$; M_{crl} = critical elastic local buckling moment; $M_{crl} = S_f\ f_{crl}$; $\lambda_d = \sqrt{(M_y / M_{crd})}$; M_{crd} = critical elastic distortional buckling moment; $M_{crd} = S_f\ f_{crd}$; $C_{yd} = \sqrt{(0.673 / \lambda_d)} \leq 3$; f_{crl} and f_{crd} are the critical elastic buckling stress for local and distortional buckling respectively that may be obtained from the elastic buckling software either *Thinwall* (Papangelis and Hancock 1995) [15] or *CUFSM* (Li and Schafer 2010) [16]. However, it should also be noted that the design Eqs. (13-21) are applicable only for the CFS beams that fall under the geometric and material limitations given in Table 1.1.1-2 of AISI (2012a) [3]. For all other CFS specimens that are not meeting the limitations of Table 1.1.1-2 of AISI (2012a) [3], a more conservative design resistance factor shall be used as per section 1.1.2 of AISI (2012a) [3].

4. Design approaches, results, and discussion

4.1 Elastic Buckling Analysis for Sheathing Braced Design

Performing the elastic buckling analysis to determine the critical elastic buckling stress or moments of the CFS test specimens is the next step after the theoretical stiffness determination if the DSM method is to be used for the strength prediction. The elastic buckling analysis was carried out using the finite-strip analysis software *CUFSM* (Li and Schafer 2010) [16]. The advantage of this software tool is that the local and distortional modes of the CFS sections can be identified by comparing the buckled shape of the CFS sections. In addition, this finite-strip analysis tool has an additional advantage of incorporating the sheathing stiffnesses obtained from Eqs. (1-12) in the elastic buckling analysis. To obtain the critical elastic buckling stress or moment that includes the effect of sheathing, the calculated stiffnesses from Table 1 should be included in the CFS structural member model at the point of sheathing fastener connections (mid-node of top and bottom flange) as shown in Fig. 1d. Since this analysis is based on the cross-sectional strip, the theoretical stiffnesses (k_x, k_y, and k_ϕ) that are calculated using the Eqs. (1, 4 and 9) need to be converted as a stiffness per unit length of the member. Therefore, these stiffnesses should be divided by the fastener spacing (d_f) to convert to uniform stiffness values along the length of the sheathed member. Hence, these stiffness values per unit length may be identified with an underline as $\underline{k_x}$, $\underline{k_y}$, and $\underline{k_\phi}$ respectively. The calculated stiffness values based on the above Eqs. (1-12) are summarized in Table 1.

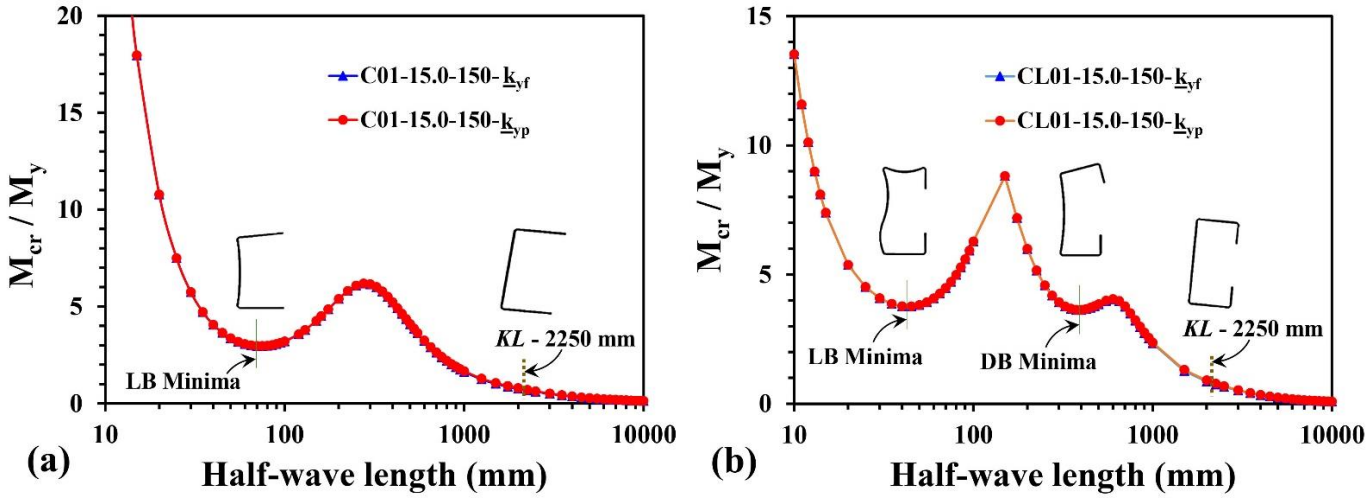

Fig. 2. Results of elastic buckling analysis: Full composite action (kyf) versus Partial composite action (kyp): (a) Sheathed Specimen C 01-15.0-150; (b) Sheathed Specimen CL 01-15.0-150

Table 1. Sheathing configurations and results of stiffness calculation at each sheathing-fastener connections

Specimen	Cross sectional dimensions of CFS stud				Sheathing configuration		Sheathing-fastener connection stiffnesses				
	Outer-to-outer Depth (h) (mm)	Outer-to-outer Breadth (b) (mm)	Depth of lip (d_l) (mm)	Thickness (t) (mm)	Sheathing thickness (t_b) (mm)	Fastener spacing (d_f) (mm)	$\underline{k}_x$ (N/mm/mm)	$\underline{k}_y$ (N/mm/mm)		$\underline{k}_\phi$ (N/mm/mm/rad)	
								$\underline{k}_{y(pc)}$	$\underline{k}_{y(fc)}$	$\underline{k}_\phi$ (T)	$\underline{k}_\phi$ (Eq) (Eq.12)
CL01-12.5-150	67.5	38	20	1.5	12.5	150	1.475	0.028	0.024	460.3	108.4
CL01-12.5-300					12.5	300	0.928	0.023	0.024	460.3	108.4
CL01-15.0-150					15.0	150	1.168	0.051	0.035	499.5	110.4
CL01-15.0-300					15.0	300	0.697	0.052	0.035	499.5	110.4
CL02-12.5-150	80	28.5	28.5	2.5	12.5	150	2.730	0.021	0.032	607.4	172.6
CL02-12.5-300					12.5	300	2.198	0.067	0.032	607.4	172.6
CL02-15.0-150					15.0	150	2.455	0.038	0.047	677.5	177.8
CL02-15.0-300					15.0	300	1.862	0.037	0.047	677.5	177.8
CL03-12.5-150	80	43.5	10	1.5	12.5	150	1.475	0.048	0.032	460.3	108.4
CL03-12.5-300					12.5	300	0.930	0.027	0.032	460.3	108.4
CL03-15.0-150					15.0	150	1.168	0.042	0.047	499.5	110.4
CL03-15.0-300					15.0	300	0.697	0.054	0.047	499.5	110.4
C01-12.5-150	50	36	-	2.5	12.5	150	2.730	0.024	0.015	607.4	172.6
C01-12.5-300					12.5	300	2.198	0.033	0.015	607.4	172.6
C01-15.0-150					15.0	150	2.455	0.038	0.022	677.5	177.8
C01-15.0-300					15.0	300	1.862	0.058	0.022	677.5	177.8
C02-12.5-150	50	45	-	1.5	12.5	150	1.475	0.036	0.015	460.3	108.4
C02-12.5-300					12.5	300	0.928	0.027	0.015	460.3	108.4
C02-15.0-150					15.0	150	1.168	0.031	0.022	499.5	110.4
C02-15.0-300					15.0	300	0.697	0.042	0.022	499.5	110.4
C03-12.5-150	80	50	-	1.5	12.5	150	1.475	0.046	0.032	460.3	108.4
C03-12.5-300					12.5	300	0.928	0.031	0.032	460.3	108.4
C03-15.0-150					15.0	150	1.168	0.038	0.047	499.5	110.4
C03-15.0-300					15.0	300	0.697	0.053	0.047	499.5	110.4
C04-12.5-150	80	50	-	2.5	12.5	150	2.730	0.039	0.032	607.4	172.6
C04-12.5-300					12.5	300	2.198	0.025	0.032	607.4	172.6
C04-15.0-150					15.0	150	2.455	0.044	0.047	677.5	177.8
C04-15.0-300					15.0	300	1.862	0.054	0.047	677.5	177.8
C05-12.5-150	50	65	-	1.5	12.5	150	1.475	0.046	0.015	460.3	108.4
C05-12.5-300					12.5	300	0.928	0.048	0.015	460.3	108.4
C05-15.0-150					15.0	150	1.168	0.050	0.022	499.5	110.4

Young's modulus (E_s) of 1.5 mm and 2.5 mm CFS studs are 210.93 GPa and 215.87 GPa respectively; Yield strength (f_y) of 1.5 mm and 2.5 mm CFS studs are 377.36 MPa and 329.9 MPa respectively ; b= breadth of flange (out-to-out); d_f= fastener spacing; h= depth of web (out-to-out); t= base metal thickness of CFS sections; t_b= sheathing thickness;

Table 2. Elastic buckling analysis results of stiffness combinations I, II and III

Specimen	Stiffness combination I "AISI's Stiffness Components" - All together approach			Stiffness combination II – "Weak axis restraint approach"			Stiffness combination III - "Rotational restraint approach"					
	k_x k_{yf} and k_ϕ (T)			k_x k_{yf}			k_{yf} k_ϕ (T)			k_{yf} k_ϕ (Eq)		
	M_{crl} / M_y	M_{crd} / M_y	M_{cre} / M_y	M_{crl} / M_y	M_{crd} / M_y	M_{cre} / M_y	M_{crl} / M_y	M_{crd} / M_y	M_{cre} / M_y	M_{crl} / M_y	M_{crd} / M_y	M_{cre} / M_y
CL01 - Un	3.76	3.62	0.57	3.76	3.62	0.57	3.76	3.62	0.57	3.76	3.62	0.57
CL01-12.5-150	3.76	3.99	11.05	3.76	3.69	9.47	3.76	3.99	1.62	3.76	3.71	1.04
CL01-12.5-300	3.76	3.97	10.81	3.76	3.67	9.12	3.76	3.97	1.62	3.76	3.71	1.04
CL01-15.0-150	3.76	4.01	11.77	3.76	3.68	9.92	3.76	4.01	1.68	3.76	3.71	1.07
CL01-15.0-300	3.76	4.00	11.22	3.76	3.66	9.14	3.76	4.00	1.68	3.76	3.71	1.07
CL02 - Un	9.84	7.43	0.69	9.84	7.43	0.69	9.84	7.43	0.69	9.84	7.43	0.69
CL02-12.5-150	9.84	7.8	27.11	9.84	7.7	25.73	9.84	7.8	1.45	9.84	7.46	1.01
CL02-12.5-300	9.84	7.76	26.1	9.84	7.65	24.49	9.84	7.76	1.45	9.84	7.46	1.01
CL02-15.0-150	9.84	7.79	27.87	9.84	7.68	26.16	9.84	7.79	1.52	9.84	7.46	1.03
CL02-15.0-300	9.84	7.74	24.5	9.84	7.63	22.45	9.84	7.74	1.52	9.84	7.46	1.03
CL03 - Un	2.86	1.64	0.48	9.84	7.43	0.69	9.84	7.43	0.69	9.84	7.43	0.69
CL03-12.5-150	2.86	1.82	11.08	2.86	1.65	9.26	2.86	1.82	1.36	2.86	1.69	0.9
CL03-12.5-300	2.86	1.82	10.63	2.86	1.65	8.77	2.86	1.82	1.36	2.86	1.69	0.9
CL03-15.0-150	2.86	1.83	11.62	2.86	1.65	9.26	2.86	1.83	1.40	2.86	1.69	0.94
CL03-15.0-300	2.86	1.83	10.45	2.86	1.65	9.55	2.86	1.83	1.4	2.86	1.69	0.94
C01 - Un	2.96	-	0.59	2.96	-	0.59	2.96	-	0.59	2.96	-	0.59
C01-12.5-150	3.00	-	5.93	3.00	-	26.03	3.00	-	2.01	3.00	-	1.22
C01-12.5-300	3.00	-	5.59	3.00	-	25.53	3.00	-	2.01	3.00	-	1.22
C01-15.0-150	3.00	-	5.81	3.00	-	27.30	3.00	-	2.12	3.00	-	1.25
C01-15.0-300	3.00	-	5.41	3.00	-	25.63	3.00	-	2.12	3.00	-	1.25
C02 - Un	0.57	-	0.42	0.57	-	0.42	0.57	-	0.42	0.57	-	0.42
C02-12.5-150	0.6	-	10.42	0.6	-	9.06	0.6	-	1.96	0.6	-	1.14
C02-12.5-300	0.6	-	10.30	0.6	-	8.78	0.6	-	1.96	0.6	-	1.14
C02-15.0-150	0.6	-	11.24	0.6	-	9.62	0.6	-	2.04	0.6	-	1.17
C02-15.0-300	0.6	-	11.04	0.6	-	9.02	0.6	-	2.04	0.6	-	1.17
C03 - Un	0.44	-	0.41	0.44	-	0.41	0.44	-	0.41	0.44	-	0.41
C03-12.5-150	0.47	-	11.79	0.47	-	9.84	0.47	-	1.32	0.47	-	0.87
C03-12.5-300	0.47	-	11.27	0.47	-	9.30	0.47	-	1.32	0.47	-	0.87
C03-15.0-150	0.47	-	12.39	0.47	-	10.19	0.47	-	1.38	0.47	-	0.91
C03-15.0-300	0.47	-	10.98	0.47	-	8.94	0.47	-	1.38	0.47	-	0.91
C04 - Un	1.49	-	0.63	1.49	-	0.63	1.49	-	0.63	1.49	-	0.63
C04-12.5-150	1.51	-	19.72	1.51	-	18.50	1.51	-	1.54	1.51	-	1.06
C04-12.5-300	1.51	-	5.25	1.51	-	17.67	1.51	-	1.54	1.51	-	1.06
C04-15.0-150	1.51	-	20.23	1.51	-	18.77	1.51	-	1.62	1.51	-	1.1
C04-15.0-300	1.51	-	5.1	1.51	-	17.00	1.51	-	1.62	1.51	-	1.1
C05 - Un	0.28	-	0.63	0.28	-	0.63	0.28	-	0.63	0.28	-	0.63
C05-12.5-150	0.30	-	5.11	0.30	-	4.25	0.30	-	2.27	0.30	-	1.45
C05-12.5-300	0.30	-	4.99	0.30	-	4.03	0.30	-	2.27	0.30	-	1.45
C05-15.0-150	0.30	-	5.44	0.30	-	4.43	0.30	-	2.38	0.30	-	1.52

Un – Unsheathed; M_y - Yield moment; M_{crl} - Critical elastic local buckling moment; M_{crd} - Critical elastic distortional buckling moment; M_{cre} - Critical elastic lateral torsional buckling moment;

Table 3. Sheathing configurations and results of stiffness calculation at each sheathing-fastener connections

Specimen	Moment (M_{EXP}) (kN mm)	Slenderness						Design predictions – Moment (kN mm)				Comparison			
		Local	Global												
		λ_l	λ_e (Un)	λ_e (k_x, k_{yf}, $k_\phi(T)$)	λ_e (k_x, k_{yf})	λ_e (k_{yf}, $k_\phi(T)$)	λ_e (k_{yf}, $k_\phi(Eq)$)	M_{DSM}^1	M_{DSM}^2	M_{DSM}^3	M_{DSM}^4	M_{EXP} / M_{DSM}^1	M_{EXP} / M_{DSM}^2	M_{EXP} / M_{DSM}^3	M_{EXP} / M_{DSM}^4
CL01-12.5-150	1516.0	0.52	1.33	0.30	0.32	0.79	0.98	2037.1	2037.1	1874.4	1656.5	0.74	0.74	0.81	0.92
CL01-12.5-300	1464.2			0.30	0.33	0.79	0.98	2037.1	2037.1	1874.4	1656.5	0.72	0.72	0.78	0.88
CL01-15.0-150	2019.1			0.29	0.32	0.77	0.97	2037.1	2037.1	1888.1	1674.3	0.99	0.99	1.07	1.21
CL01-15.0-300	1856.8			0.30	0.33	0.77	0.97	2037.1	2037.1	1888.1	1674.3	0.91	0.91	0.98	1.11
CL02-12.5-150	2874.7	0.32	1.21	0.19	0.20	0.83	1.00	3073.3	3073.3	2760.4	2472.6	0.94	0.94	1.04	1.16
CL02-12.5-300	2596.9			0.20	0.20	0.83	1.00	3073.3	3073.3	2760.4	2472.6	0.84	0.84	0.94	1.05
CL02-15.0-150	3614.0			0.19	0.20	0.81	0.99	3073.3	3073.3	2788.8	2492.0	1.18	1.18	1.3	1.45
CL02-15.0-300	3046.7			0.20	0.21	0.81	0.99	3073.3	3073.3	2788.8	2492.0	0.99	0.99	1.09	1.22
CL03-12.5-150	1827.3	0.59	1.44	0.30	0.33	0.86	1.05	2632.6	2426.0	2323.6	2022.3	0.69	0.75	0.79	0.9
CL03-12.5-300	1858.9			0.31	0.34	0.86	1.05	2632.6	2426.0	2323.6	2022.3	0.71	0.77	0.8	0.92
CL03-15.0-150	2865.1			0.29	0.33	0.84	1.03	2632.6	2426.0	2346.6	2057.7	1.09	1.18	1.22	1.39
CL03-15.0-300	2500.6			0.31	0.32	0.84	1.03	2632.6	2426.0	2346.6	2057.7	0.95	1.03	1.07	1.22
C01-12.5-150	1598.8	0.57	1.30	0.41	0.19	0.70	0.89	1637.5	1674.3	1568.5	1406.1	0.98	0.95	1.02	1.14
C01-12.5-300	1559.4			0.42	0.20	0.70	0.89	1637.5	1674.3	1568.5	1406.1	0.95	0.93	0.99	1.11
C01-15.0-150	2225.1			0.41	0.19	0.68	0.88	1637.5	1674.3	1580.7	1413.9	1.36	1.33	1.41	1.57
C01-15.0-300	1838.9			0.42	0.19	0.68	0.88	1637.5	1674.3	1580.7	1413.9	1.12	1.1	1.16	1.3
C02-12.5-150	1221.9	1.31	1.52	0.31	0.33	0.71	0.93	1010.3	1042.1	979.4	901.4	1.21	1.17	1.25	1.36
C02-12.5-300	1247.0			0.31	0.33	0.71	0.93	1010.3	1041.4	979.4	901.4	1.23	1.2	1.27	1.38
C02-15.0-150	1510.2			0.30	0.32	0.70	0.92	1010.3	1043.3	983.2	906.3	1.49	1.45	1.54	1.67
C02-15.0-300	1249.3			0.30	0.33	0.70	0.92	1010.3	1042.0	983.2	906.3	1.24	1.2	1.27	1.38
C03-12.5-150	2242.5	1.49	1.54	0.29	0.32	0.86	1.06	1794.7	1847.8	1648.3	1496.0	1.25	1.21	1.36	1.5
C03-12.5-300	1945.8			0.30	0.33	0.86	1.06	1794.7	1845.8	1648.3	1496.0	1.08	1.05	1.18	1.3
C03-15.0-150	2566.9			0.28	0.31	0.85	1.04	1794.7	1849.0	1659.5	1515.6	1.43	1.39	1.55	1.69
C03-15.0-300	2459.5			0.30	0.33	0.85	1.04	1794.7	1844.3	1659.5	1515.6	1.37	1.33	1.48	1.62
C04-12.5-150	3415.6	0.81	1.25	0.22	0.23	0.80	0.96	3773.7	3994.2	3539.6	3183.3	0.91	0.86	0.96	1.07
C04-12.5-300	3452.5			0.43	0.24	0.80	0.96	3773.7	3992.2	3539.6	3183.3	0.91	0.86	0.98	1.08
C04-15.0-150	3521.0			0.22	0.23	0.78	0.95	3776.0	3994.8	3568.5	3222.7	0.93	0.88	0.99	1.09
C04-15.0-300	3308.1			0.44	0.24	0.78	0.95	3776.0	3990.5	3568.5	3222.7	0.88	0.83	0.93	1.03
C05-12.5-150	2346.1	1.87	1.25	0.44	0.48	0.66	0.83	1098.7	1101.2	1081.1	1025.1	2.14	2.13	2.17	2.29
C05-12.5-300	2362.2			0.45	0.50	0.66	0.83	1098.7	1098.4	1081.1	1025.1	2.15	2.15	2.18	2.30
C05-15.0-150	2645.9			0.43	0.47	0.64	0.81	1100.8	1103.2	1087.8	1035.2	2.40	2.40	2.43	2.56
Mean (P_m)												1.15	1.14	1.23	1.35
COV (V_p)												0.361	0.360	0.332	0.305
Reliability index (β_1)												1.98	1.97	2.26	2.65
Reliability index (β_2)												1.99	1.97	2.27	2.66

$\lambda_l = (f_y / f_{crl})^{0.5}$; $\lambda_e = (f_y / f_{cre})^{0.5}$; Un – Unsheathed; M_{DSM}^1- Design strength using Combination I – "AISI's Stiffness Components" - k_x, k_{yf} and k_ϕ (Eq) - All together approach;

M_{DSM}^2- Design strength using Combination II - "Sheathing Stiffness Components - weak axis restraint" – k_x and k_{yf};

M_{DSM}^3- Design strength using Combination III - "Sheathing Stiffness Components - Flexural" - k_y and k_ϕ (T);

M_{DSM}^4- Design strength using Combination III - "Sheathing Stiffness Components - Flexural" - k_y and k_ϕ (Eq);

4.2 Full-composite action ($\underline{k}_{yf}$) vs. partial composite action ($\underline{k}_{yp}$)

To begin correctly, it is necessary to examine the appropriateness of the stiffness values and choose the right one for the design before analyzing each sheathing configurations (sheathing thickness and fastener spacing). The different stiffness values obtained for full composite ($\underline{k}_{yf}$) and partial composite actions ($\underline{k}_{yp}$) in the vertical translational stiffness ($\underline{k}_{y}$) are examined. The results indicate that the differences between elastic buckling curves of $\underline{k}_{yp}$ and $\underline{k}_{yf}$ are insignificant. Figs. 2(a-b) shows a comparison between elastic buckling analysis results obtained using partial ($\underline{k}_{yp}$) and full composite action ($\underline{k}_{yf}$) for specimen C01-15.0-150 and CL01-15.0-150, where the curves are identical with one on top of the other. It should be noted that in the comparison study between the partial ($\underline{k}_{yp}$) and full composite action ($\underline{k}_{yf}$), the other sheathing stiffnesses ($\underline{k}_{x}$, $\underline{k}_{\phi}$) are not included as described in the Fig. 2 (see legends). Therefore, to maintain consistency, the full composite action stiffnesses ($\underline{k}_{yf}$) arrived from Eqs. (4, 7 and 8) was used in all elastic buckling analysis. As described previously in the introduction section, the different combinations of sheathing stiffnesses were used in the design strength prediction work as follows;

4.3 Combination I – "AISI's Stiffness Components" - $\underline{k}_{x}$, $\underline{k}_{y,}$ and $\underline{k}_{\phi}$ - All together approach (M_{DSM}^{1})

After adopting full composite action ($\underline{k}_{yf}$) as the appropriate composite action between the sheathing and CFS member, the other sheathing stiffnesses ($\underline{k}_{x}$, $\underline{k}_{\phi}$) needs to be incorporated together with $\underline{k}_{yf}$ in the elastic buckling analysis. It should be noted that the $\underline{k}_{\phi}$ (T) values calculated from the $\underline{k}_{\phi c}$ values obtained from the Table Z.1-2[1] of AISI [2] are used in the first stiffness combination. Therefore, for the first elastic buckling analysis, the stiffness combination is $\underline{k}_{x}$, $\underline{k}_{yf,}$ and $\underline{k}_{\phi}$ (T) (Fig. 3a). The signature curves obtained from the elastic buckling analysis is shown in Fig. 3c (plain C channel) and Fig. 3d (C channel with a lip) for both unsheathed and sheathed (with $\underline{k}_{x}$, $\underline{k}_{yf,}$ and $\underline{k}_{\phi}$ (T)) CFS studs. In general, the elastic buckling analysis results indicate that the presence of sheathing has significantly improved the elastic buckling stress thereby elastic moments. The values of critical elastic buckling moments ($M_{cre,}$ $M_{crl,}$ and M_{crd}) obtained from the elastic buckling analysis are shown in Table 2 as a ratio to its corresponding yield moment (M_y). The critical elastic buckling moments of local and distortional buckling (M_{crl} and M_{crd}) were obtained from the minima shown in the elastic buckling curves (Figs. 3(c and d)), but the global critical elastic buckling stress (M_{cre}) values were picked for the half wavelength of 2250 mm. The half wavelength was calculated by multiplying the center to center distance of the tested specimen with the effective length coefficient (K) from the Table C-C4.1-1 of AISI S100 Commentary (AISI 2012c) [18]. The value of effective length coefficient is unity (K=1) as per AISI (2012c) [18] for the simply supported conditions.

In the elastic buckling analysis of sheathed member design, even though the midpoint of the flange was added with a rotational and vertical stiffness (k_{ϕ} and k_{y}) which was supposed to arrest the buckling of the CFS flange element, the local buckling stresses of the CFS stud did not improve for specimens examined as shown in Figs. 3(c-d). This may be attributed to one of the following; i) local buckling was influenced by the web which was not included with restraint (stiffness), ii) shorter buckling wavelengths typically have little influence on the end conditions and restraints (Vieira and Schafer 2012a) [9] else, iii) the gypsum sheathing is not offering sufficient restraint that can arrest the local buckling modes. Even though the above points seem logical for no influence of sheathing on local buckling resistance, this occurrence of local buckling in elastic buckling analysis using the finite strip software is realistic and is conservative as well, because, in reality, the occurrence of local buckling is possible between the sheathing fastener connections. Therefore, it can also be concluded that the contribution of sheathing stiffnesses can be ignored in the design predictions if the governing failure mode (local buckling strength << distortional buckling and global buckling strength) or the governing slenderness (λ_l >>1) of the unsheathed CFS stud is local buckling and the sheathing provided is of gypsum.

In case of distortional buckling, the effect of sheathing was influential as shown in Fig. 3d. The sheathing decreased [400mm (CL 01 - Unsheathed) to 350mm (mean - CL 01 - Sheathed)] the half wavelength of the distortional buckling thereby increased the buckling strength. The global buckling strength also increased significantly due to the presence of sheathing as shown in Figs. 3(c-d). For all the specimens examined, the elastic buckling analysis results indicate that the sheathing stiffnesses ($\underline{k}_{x}$, $\underline{k}_{yf,}$ and $\underline{k}_{\phi}$ (T)) included has completely restrained the lateral torsional buckling and forced the member to undergo strong axis bending as shown in Fig. 3b with failure due to yielding (M_{cre} > 2.78 M_y). Figures 3(c-d) show that the critical elastic lateral torsional buckling strength (M_{cre}) is higher than the M_y value at the half wavelength of 2250 mm which hindered the LTB of the sheathed CFS stud. The above elastic buckling analysis results were incorporated in the DSM, and the flexural strength predicted (M_{DSM}^{1}) for each CFS sheathed panel is summarized in Table 3.

In general, the elastic buckling analysis results indicate that the M_{cre} / M_y is more than 2.78 for all the test specimens as shown in Table 2. Therefore, according to section 1.2.2.1.1.1.1 of AISI (2012a) [3], the CFS specimen will be considered as laterally braced, and the nominal flexural strength (M_{ne}) is taken as equal to yield moment (M_y) (Eq. (16)). This leads to the consideration of inelastic reserve

strength for local and distortional buckling design strength based on Eq. (18) and Eq. (20). The design results were compared with the experimental moments (M_{EXP}), and the results indicate that the design moments (M_{DSM}^1) are unconservative (M_{EXP}/M_{DSM}^1 <1) for many tested specimens as shown in Figs. 4 and 5 (dotted straight line with hollow triangle markings (M_{DSM}^1) is higher than the experimental ultimate moment (M_{EXP}) of many sheathed specimens) and conservative (M_{EXP}/M_{DSM}^1 >1) only for the specimens that are locally slender (λ_l>1) as shown in Table 3 (see specimen sets C02, C03, and C05). This unconservative design strength prediction may be due to the overestimation of nominal flexural strength (M_{ne}) as equal to the yield moment (M_y) in design as per Eq. (16) while the bending test results indicate that the sheathed specimens failed in LTB due to the pull-through failure of the screws at the sheathing-fastener connections. The consideration of yield moment in the nominal flexural strength (M_{ne}) is perhaps due to the exaggerated sheathing stiffness as a result of simultaneous application $\underline{k}_x$, $\underline{k}_y$ and $\underline{k}_\phi$ thereby not depicting the realistic sheathing effect resulting in M_{cre} value higher than 2.78 times of M_y. It should be noted that in Table 2, the C05 specimen sets values of (M_{EXP}/M_{DSM}^1), (M_{EXP}/M_{DSM}^2), (M_{EXP}/M_{DSM}^3) and (M_{EXP}/M_{DSM}^4) are higher than 2, which indicates that the DSM prediction is overly conservative for the specimens which are highly slender (λ_l >> 1). Similar observations on over conservativeness of the DSM are observed in Wang and Young [19] and Selvaraj and Madhavan [8].

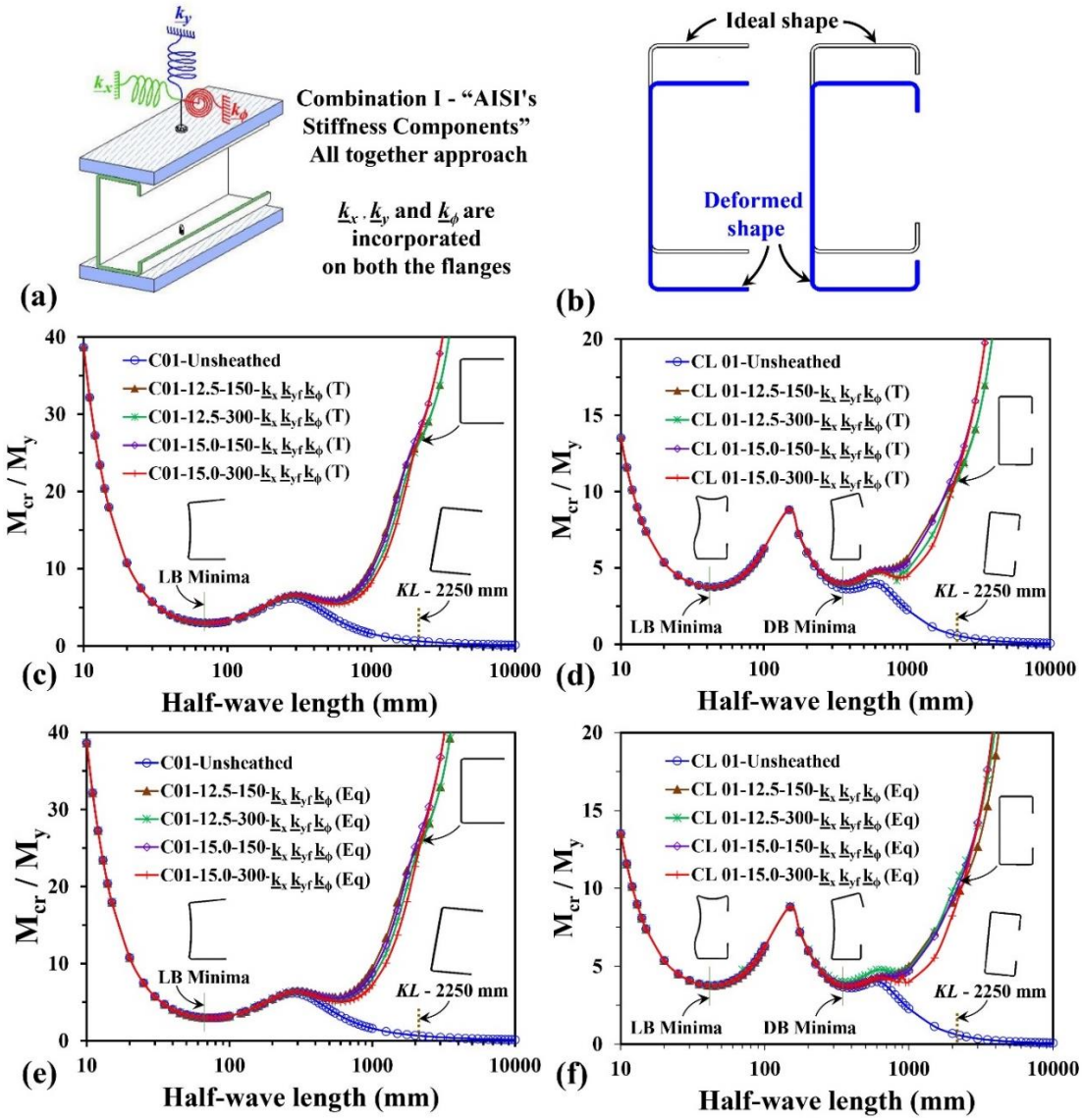

Fig. 3. Results of elastic buckling analysis: Combination I - "AISI's Stiffness Components" - kx, ky and kϕ - All together approach: (a) Stiffnesses input; (b) Elastic buckling failure modes (c) Sheathed Specimen set C 01; (d) Sheathed Specimen set CL 01

To further confirm the above statement on the unconservative prediction of design strength, the lower bound values for connection rotational stiffness ($k_{\phi c}$) using the Eq. (12) in the rotational stiffness $\underline{k}_{\phi}$ (*Eq*) (Eq. 9) was used in the elastic buckling analysis in place of $\underline{k}_{\phi}$ *(T)*. The results obtained from the elastic buckling analysis shown in Fig. 3e (plain C channel) and Fig. 3f (C channel with a lip) and it indicates that the difference between the design strengths using $\underline{k}_{\phi}$ (*Eq*) and $\underline{k}_{\phi}$ (T) is insignificant and hence it is obvious that the design strength will remain same and unconservative (M_{EXP} /M_{DSM} <1). Such unconservative design outcome has led to reinvestigate the stiffness components that are incorporated in the elastic buckling analysis.

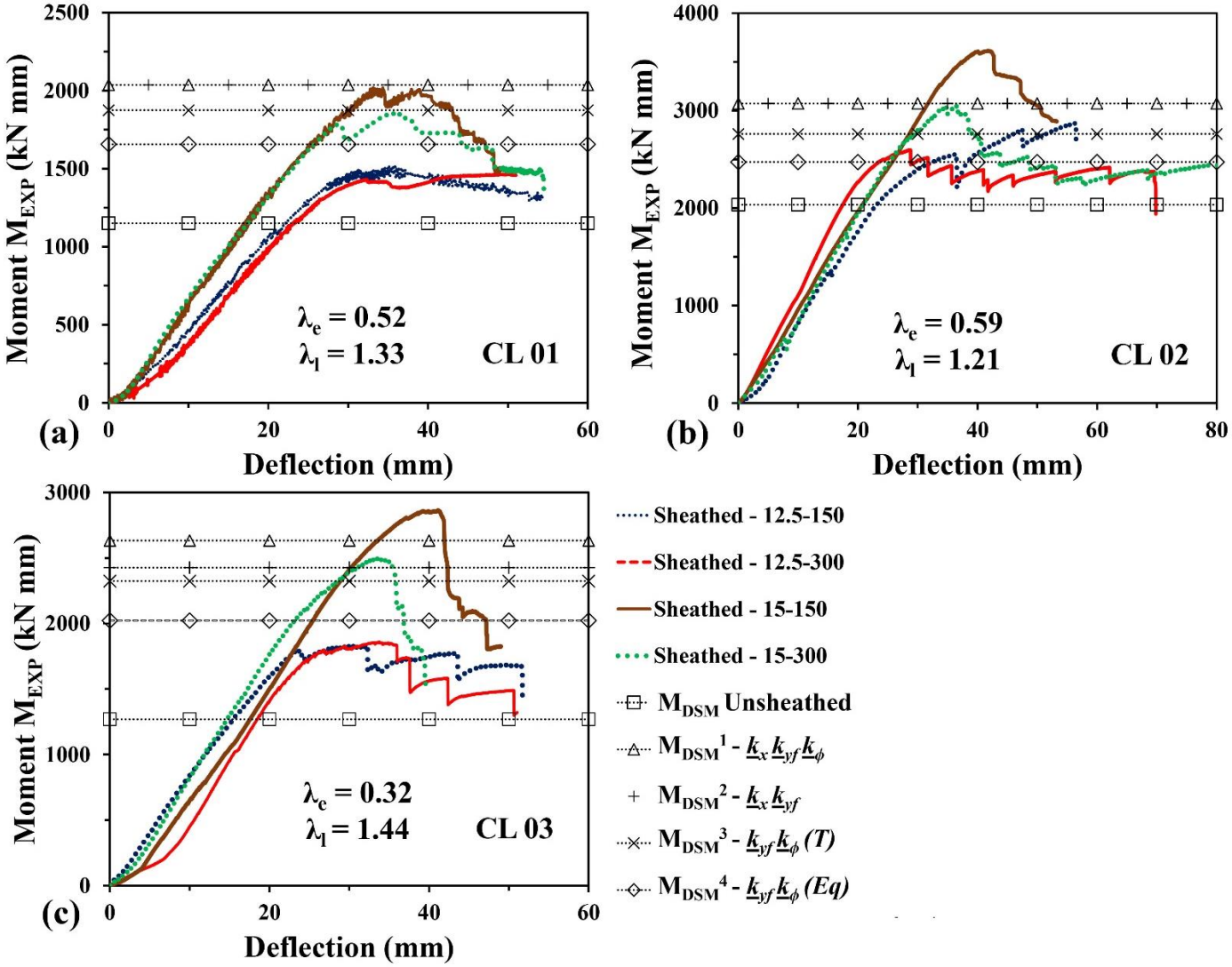

Fig. 4. Comparison of design strength predictions (M_{DSM}) with experimental results (M_{EXP}): (a) Sheathed Specimen set CL 01; (b) Sheathed Specimen set CL 02: (c) Sheathed Specimen set CL 03

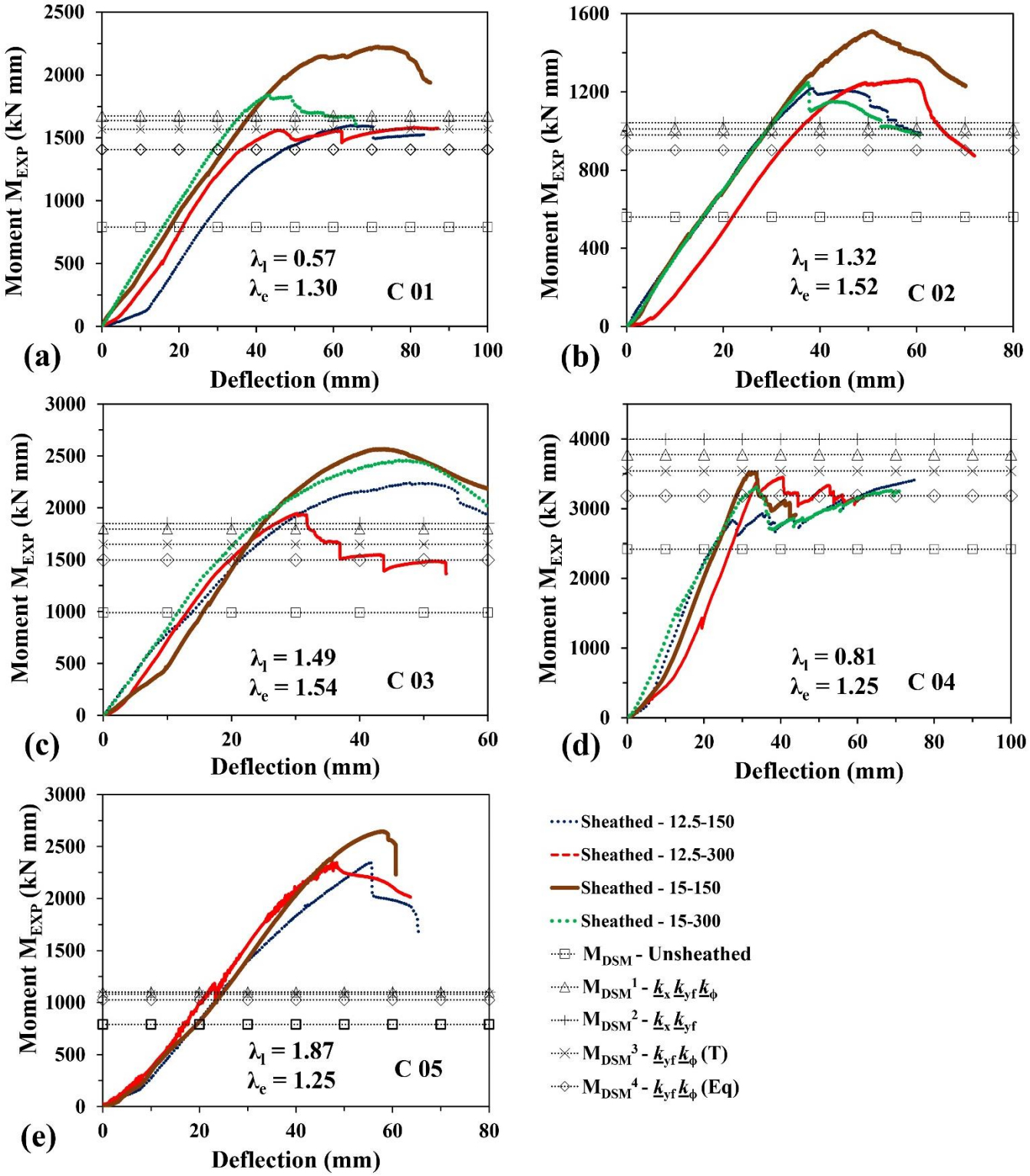

Fig. 5. Comparison of design strength predictions (M_{DSM}) with experimental results (M_{EXP}): (a) Sheathed Specimen set C 01; (b) Sheathed Specimen set C 02; (c) Sheathed Specimen set C 03; (d) Sheathed Specimen set C 04; (e) Sheathed Specimen set C 05

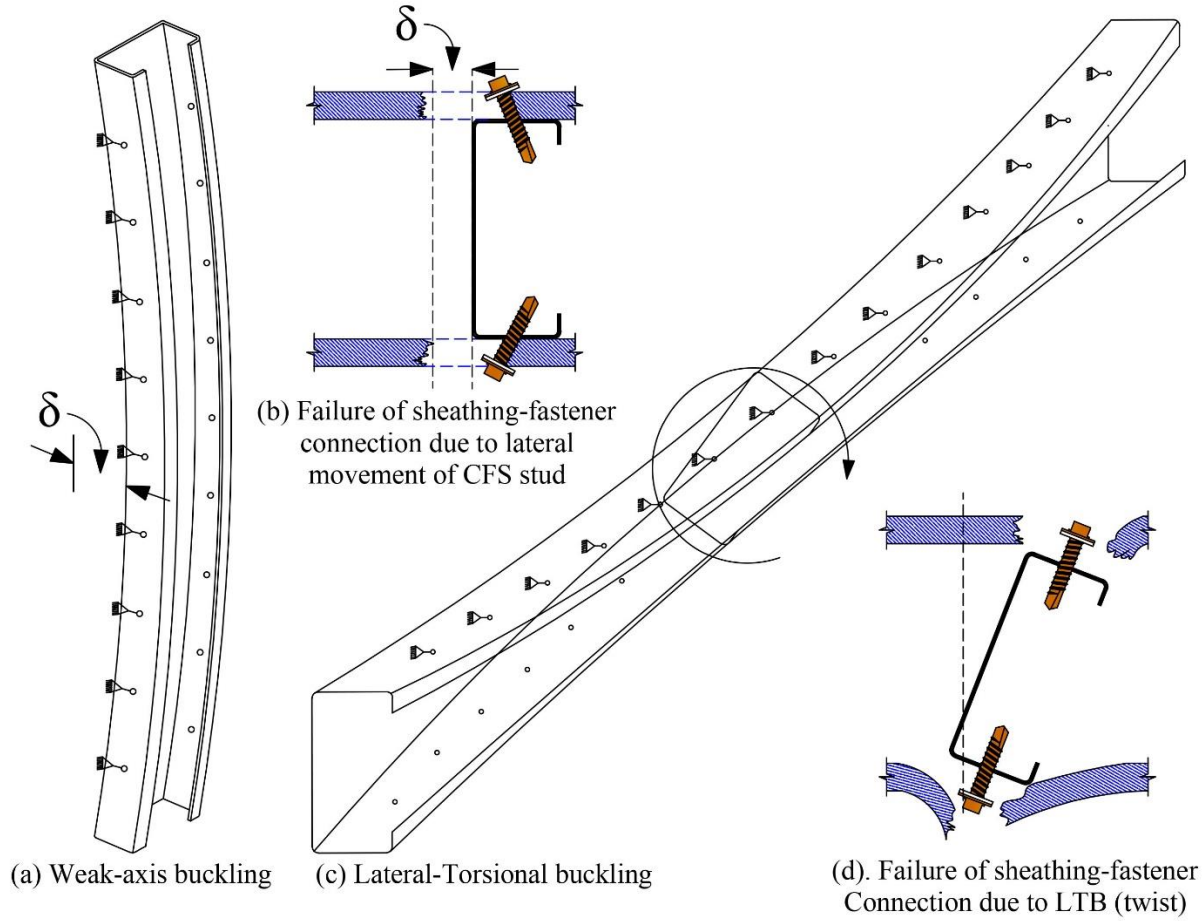

Fig.6. Sheathing restraint - Comparison – Axial compression versus Flexural loading

The structural member subjected to bending will fail in yielding only if they are laterally restrained or has very low slendernesses (global and local). In the present study, the incorporation of all the stiffnesses ($\underline{k}_x$, $\underline{k}_{yf,}$ and $\underline{k}_\phi$) in the sheathed CFS specimen prevented LTB type failure and resulted in failure due to yield. Therefore, it is necessary to examine the accuracy and appropriateness of the input parameters namely the stiffnesses (vertical, translational and rotational) and in particular the way in which the expressions (mechanics involved in the experimental setup) for each stiffness were derived and the appropriate choice of stiffness components that will reflect the reality in the design of sheathed specimens that are subjected to bending.

Lateral translational stiffness (k_x): This stiffness can be defined as the resistance offered by the sheathing against the shear force developed at each sheathing fastener connection when the CFS stud in the sheathed panel moves in the lateral direction alone (Fig. 6a) due to the weak axis buckling. Therefore, the test setup developed by Winter (1960) [4] resembles the same by applying the pulling force to the identically sheathed CFS studs assembled in parallel as shown in Fig. 6b and the total shear developed at each sheathing fastener connection is equivalent to the force applied.

Rotational stiffness (k_ϕ): This stiffness can be defined as the resistance offered to the cross-sectional twist or rotation of the flange attached to the sheathing (Fig. 6c). This stiffness will be very small if the sheathing material is soft (for example gypsum boards). Therefore, failure of this stiffness will result in a pull through failure at sheathing fastener connection as shown in Fig. 6d.

In addition, it should be noted that the lateral translational stiffness (k_x) and rotational stiffness (k_ϕ) were derived from different experimental test setups. Basically, the lateral translational stiffness (k_x) prevents the weak axis bending, and rotational stiffness (k_ϕ) prevents the cross-sectional twist. However, in reality, among the global buckling failure modes, either the weaker axis buckling or LTB (cross-sectional twist) would occur. Hence, simultaneous application of both these lateral translational stiffness (k_x)

and rotational stiffness (k_ϕ) is akin to double dipping since the sheathing stiffness is accounted twice thereby fictitiously increasing the sheathing stiffness leading to complete elimination of LTB (twist) and lateral movement (weak axis) resulting in unconservative design results. Therefore, the appropriate one, either k_x or k_ϕ should be selected to achieve the failure mode similar to experimental results.

4.4 Combination II - "Sheathing Stiffness Components - weak axis restraint" – $\underline{k}_x$ and $\underline{k}_y$ (Improved approach) (M_{DSM}^2)

In the second combination of stiffnesses, the lateral translational stiffness ($\underline{k}_x$) and vertical stiffness ($\underline{k}_y$) have been used as shown in Fig. 7a. The elastic buckling results of the second combination of stiffnesses are shown in Fig. 7c (plain C channel) and Fig. 7d (C channel with a lip) for both the unlipped and lipped C channels. The results indicate that the difference between the first combination and second combination results are insignificant and the elastic buckling analysis failure mode is still major axis buckling with yielding (see Fig. 7b) as in combination I (Fig. 3b). Therefore, the design moments (M_{DSM}^2) calculated using the second combination of stiffness is almost equal to the design moments of first design approach (M_{DSM}^1) using all the stiffnesses [($M_{DSM}^2 \approx M_{DSM}^1$)>$M_{EXP}$] as shown in Table 3 and Figs. 4-5 [dotted straight line with hollow triangles markings (M_{DSM}^1) and dotted straight lines with **"+"** markings (M_{DSM}^2) are almost same]. These results further indicate that the $\underline{k}_x$ is the one which restraints the lateral movement of the CFS stud and ensures failure due to yielding in the sheathed panel specimen. Hence, to allow cross-section twist (translation of flanges in the opposite direction), the lateral translational stiffness ($\underline{k}_x$) need to be ignored from the elastic buckling analysis necessary for predicting the flexural design strength of sheathed CFS panels.

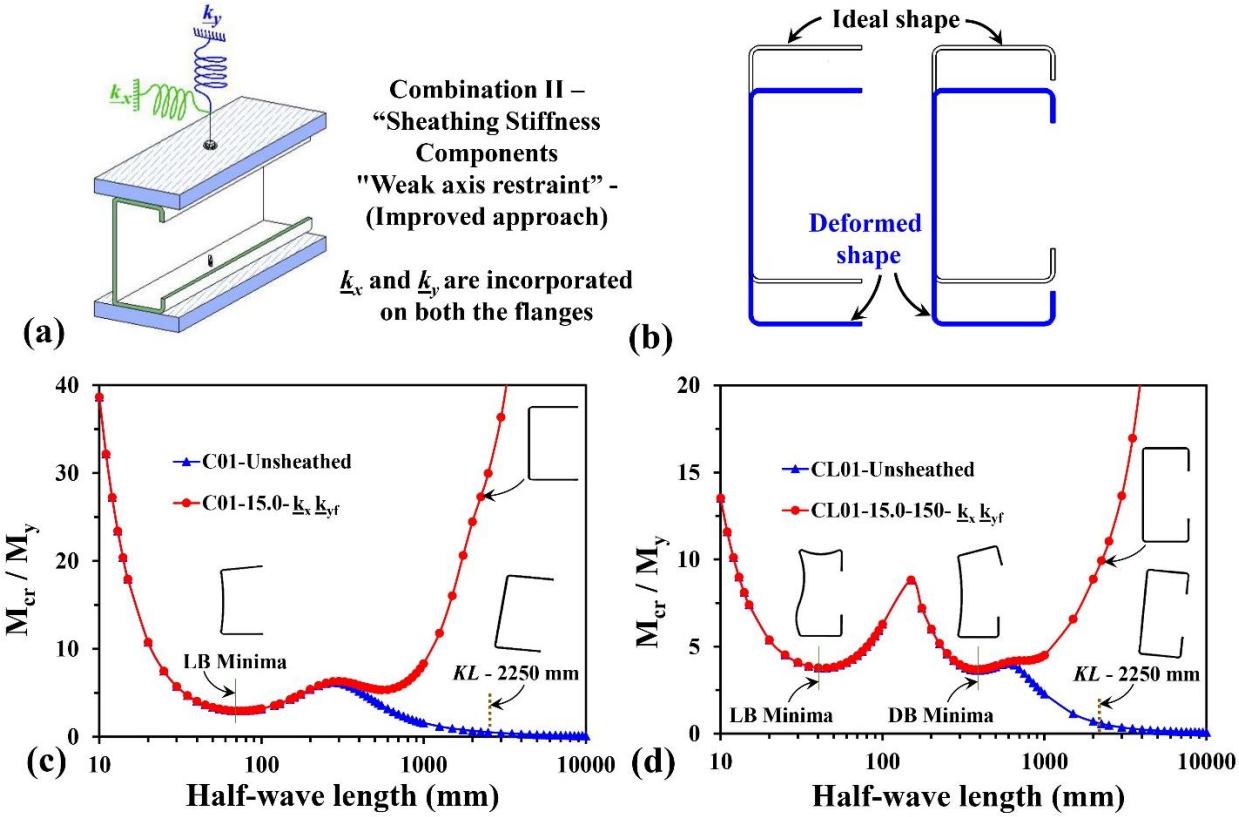

Fig. 7. Results of elastic buckling analysis: Combination II - "Sheathing Stiffness Components - weak axis restraint" – kx and ky (Improved approach): (a) Stiffnesses input; (b) Elastic buckling failure modes (c) Sheathed Specimen set C 01; (d) Sheathed Specimen set CL 01

4.5 Combination III - "Sheathing Stiffness Components - Flexural" - $\underline{k}_y$ and $\underline{k}_\phi$ (Improved approach) (M_{DSM}^3 and M_{DSM}^4)

The third and improved combination of stiffness components consists of only two stiffnesses ($\underline{k}_y$ and $\underline{k}_\phi$), after ignoring the lateral translational stiffness (k_x) as shown in Fig. 8a. The Fig. 8c (plain C channel) and Fig. 8d (C channel with a lip) shows the results of elastic buckling analysis (signature curves) with $\underline{k}_{yf}$ and $\underline{k}_\phi$ (T). The results show a significant decrease [at the half wavelength of 2250 mm in Figs. 8(c-d)] compared to the previous elastic buckling results using AISI's "all together approach" ($\underline{k}_x$, $\underline{k}_{yf}$, and $\underline{k}_\phi$) [Figs. 3(c-f)]

and the approach using stiffness combination II ($\underline{k}_x$ *and* $\underline{k}_y$) [Figs. 7(c-d)]. In addition, the elastic buckling failure mode in combination III also indicates that the failure was due to LTB (lateral displacement with a twist) as shown in Fig. 8b which is similar to the experimental failure modes. The obtained values of M_{cre}/M_y for each sheathed specimens from the elastic analysis using $\underline{k}_{yf}$ and $\underline{k}_\phi$ (T) is summarized in Table 2. The corresponding design moment ($M_{DSM}{}^3$) determined also indicate that mean value of $M_{EXP}/M_{DSM}{}^3$ is 1.23, and the results are found to be mostly conservative as shown in Table 3. Therefore, ignoring the translational stiffness $\underline{k}_x$ in the flexural design of sheathed CFS members' results in a reasonable prediction of design strength. In addition, the use of the lower bound value of $\underline{k}_\phi$ *(Eq)* in place of $\underline{k}_\phi$ (*T*) in the combination III indicates a closer comparison with the experimental results as shown in Table 3 (mean of $M_{EXP}/M_{DSM}{}^4$ = 1.35).

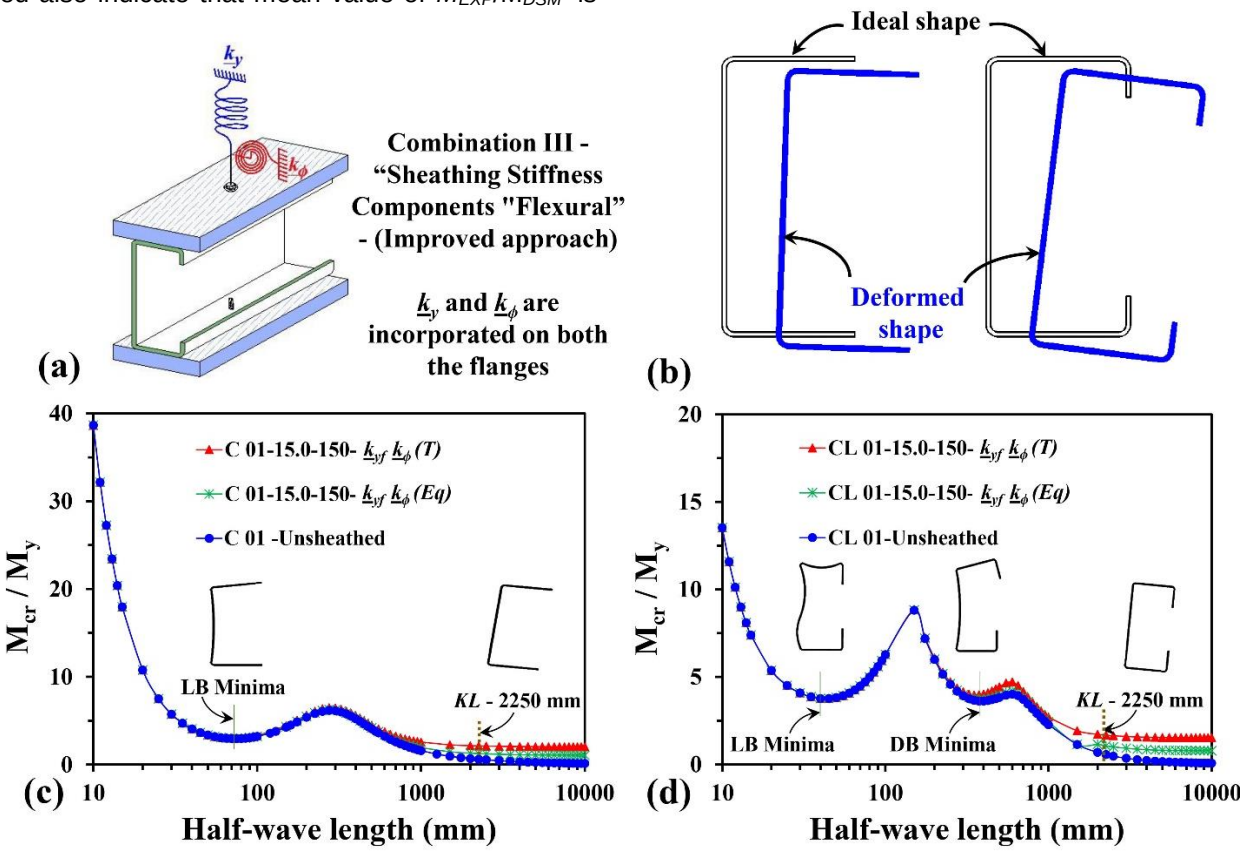

Fig. 8. Results of elastic buckling analysis: Combination III - "Sheathing Stiffness Components - Flexural" - ky and kϕ (Improved approach): (a) Stiffnesses input; (b) Elastic buckling failure modes (c) Sheathed Specimen set C 01; (d) Sheathed Specimen set CL 01

The nominal design strength of sheathed members determined based on the above approach (Stiffness combination III) was compared with the ultimate loads obtained from the results of the experiment as shown Figs. 4-5 [compare the dotted line with a legend "$M_{DSM}{}^4$ – k_{yf} k_ϕ *(Eq)*" and ultimate moment (M_{EXP}) in each curve]. It was observed that the design results are unconservative only for the 4 specimens (CL01-12.5-150, CL01-12.5-300, CL03-12.5-150, and CL03-12.5-300) by approximately 10% of the 31 specimens tested as shown in a column titled "Comparison - M_{EXP} / $M_{DSM}{}^4$" of Table 3. However, the unconservativeness may be compensated by appropriately adjusting the design resistance factors (ϕ_b) (AISI 2012a) [3]. In addition, the comparison of test results with the predicted moment capacities is also plotted in Fig. 9 with respect to the corresponding global slenderness values obtained from design approaches adopted. Figure 9 shows that the improved design approach using the sheathing stiffnesses ($\underline{k}_y$ and $\underline{k}_\phi$ (*Eq*)) ($M_{DSM}{}^4$) is conservative with the test results, while the "all together approach" ($\underline{k}_x$, $\underline{k}_y$, and $\underline{k}_\phi$) by AISI (2013a) [2] ($M_{DSM}{}^1$) is unconservative since it overestimates the sheathing stiffnesses and reduces the slenderness of the member significantly as shown in Table 3. The design curves "AISI-2012 - Unbraced" and "AISI-2012 - braced" in Fig. 9 represents the design strength predictions for the lateral unrestrained beam (M_{cre} < 2.78 M_y) and laterally restrained beam (M_{cre} > 2.78 M_y) using AISI 2012 [3].

5. Reliability analysis

The reliability analysis was performed for both "AISI's Stiffness Components" ($\underline{k}_x$, $\underline{k}_y$, and $\underline{k}_\phi$ - All together

approach) and "Sheathing Stiffness Components - Flexural" ($\underline{k}_y$ and $\underline{k}_\phi$ -Improved approach) methods to check the adaptability of them in the design specifications. The ultimate experimental moment capacities (M_{EXP}) of the sheathed CFS panels subjected to out-of-plane bending were compared with the nominal moment capacities (M_{DSM}) determined using various design methods adopted as shown in Table 3. The bending coefficient (C_b) was conservatively taken as unity (C_b=1.0) in the design calculations based on the approach adopted by Niu et al. (2014). Two different load combinations were used in the reliability index calculations specified in ASCE (2010) [20] and AS/NZS (2002) [21] as 1.2 D+1.6 L and 1.2 D + 1.5 L respectively, where D is the dead load and L is the live load. The statistical parameters used (V_f = 0.05, F_m = 1.00, V_m = 0.10 and M_m = 1.1) for the calculation of reliability index is given in Table F1 of AISI (2012a) [3] and the mean values of M_{EXP} / M_{DSM} (P_m) and coefficient of variation values (V_p) for the corresponding design methods are shown in Table 3. In addition, the resistance factor (ϕ_b) values of 0.9 and 0.8 are used for prequalified beams and beams that does not come under the limitations as per Table 1.1.1.2 in Appendix 1 of AISI S100-12 [3] respectively AISI [3]; Wang and Young [19].

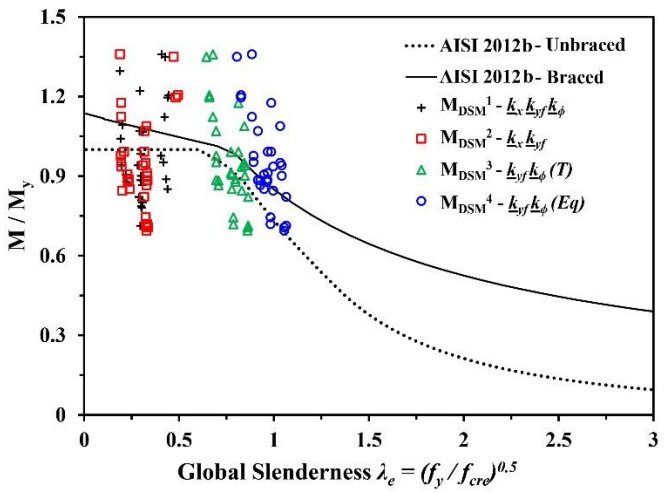

Fig. 9. Comparison of different design approaches – Design methods for sheathed CFS structural members

The results of the reliability index calculations indicates that the "AISI's Stiffness Components" ($\underline{k}_x$, $\underline{k}_y$, and $\underline{k}_\phi$ - All together approach) method's reliability index value for both the load combinations adopted (β_1 and β_2 =1.8) is less than the target reliability index (β_o=2.5) value specified for the structural members for the LFRD design as per section F1. 1(c) of AISI S100-12 [3]. The reliability index values determined for the newly improved design approach "Sheathing Stiffness Components - Flexural" ($\underline{k}_y$ and $\underline{k}_\phi$ (*Eq*)) for both the load combinations of ASCE (2010) [20] and AS/NZS (2002) [21] exceeds (β_1 = 2.65 and β_2 = 2.66) the target reliability index value (β_o=2.5) as shown in Table 3. Therefore, the improved design approach using the sheathing stiffness ($\underline{k}_y$ and $\underline{k}_\phi$ (*Eq*)) is found to be accurate in terms of both design strength and failure modes as well as probalistically reliable for the design of sheathed CFS members subjected to out-of-plane loadings. In addition, it should be noted that the design strength calculation results indicate that the flexural strength of the member increased by a maximum of 62.2% compared to the unsheathed design strength (M_{DSM} -Unsheathed) as shown in Table 4.

6. Conclusions

Design strength calculations for the sheathed CFS panels subjected to out-of-plane bending is performed for the various sheathing stiffness combinations. Various parameters such as slenderness of the CFS stud, sheathing thickness, and fastener spacing were examined through design. In general, the design results indicates that the contribution of sheathing stiffnesses can be ignored in the design predictions if the governing failure mode (local buckling strength << distortional buckling and global buckling strength) or the governing slenderness (λ_l >>1) of the unsheathed CFS stud is local buckling and the sheathing provided is of gypsum.

A comparison of the experimental results with the predicted strengths using the current design approach available in the AISI (2013a) [2] indicates that the results are unconservative for a majority of the sheathed panels investigated in this study. This is due to the fact that the AISI (2013a) [2] recommends the simultaneous application of all the stiffness components ($\underline{k}_x$, $\underline{k}_y$, and $\underline{k}_\phi$) which is a key input inelastic buckling analysis irrespective of loading conditions for determining the design strength of sheathed CFS panels.

An in-depth analysis on the stiffnesses provided by sheathing-fastener connections indicates that the inclusion of lateral stiffness ($\underline{k}_x$) inhibits the natural failure mode (LTB) exhibited by the test specimens due to excessive lateral restraint. A modified approach by using $\underline{k}_y$ and $\underline{k}_\phi$ (*Eq*) that is presented as an alternative to the existing AISI's "all together approach" ($\underline{k}_x$, $\underline{k}_y$, and $\underline{k}_\phi$) provides design strengths and failure modes that are in good comparison with the experimental results. The reliability studies carried out also indicates that proposed modified approach can be adopted in AISI for sheathed member design subjected to flexure.

In addition to the above modified approach, the authors of this paper have now developed a new design approach called "Direct Stiffness-Strength Approach" in the companion paper titled "Sheathing Braced Design of CFS Studs using Direct Stiffness-Strength Method Design" in this conference [22]. More details about the Direct Stiffness-Strength Method shall be obtained from the following papers [23-38].

Table 4. Increased design strength due to sheathing

Specimen	Design predictions - Moment (kN mm) strength (kN mm)		Increased design strength in %
	M_{DSM} - Unsheathed	$M_{DSM}{}^{4}$ - Sheathed	
CL01-12.5-150	1150.6	1656.5	44.0
CL01-12.5-300		1656.5	44.0
CL01-15.0-150		1674.3	45.5
CL01-15.0-300		1674.3	45.5
CL02-12.5-150	2034.5	2472.6	21.5
CL02-12.5-300		2472.6	21.5
CL02-15.0-150		2492.0	22.5
CL02-15.0-300		2492.0	22.5
CL03-12.5-150	1268.7	2022.3	59.4
CL03-12.5-300		2022.3	59.4
CL03-15.0-150		2057.7	62.2
CL03-15.0-300		2057.7	62.2
C01-12.5-150	966.82	1406.1	45.4
C01-12.5-300		1406.1	45.4
C01-15.0-150		1413.9	46.2
C01-15.0-300		1413.9	46.2
C02-12.5-150	560.02	901.4	61.0
C02-12.5-300		901.4	61.0
C02-15.0-150		906.3	61.8
C02-15.0-300		906.3	61.8
C03-12.5-150	990.25	1496.0	51.1
C03-12.5-300		1496.0	51.1
C03-15.0-150		15156	53.1
C03-15.0-300		1515.6	53.1
C04-12.5-150	2416.9	3183.3	31.7
C04-12.5-300		3183.3	31.7
C04-15.0-150		3222.7	33.3
C04-15.0-300		3222.7	33.3
C05-12.5-150	790.29	1025.1	29.7
C05-12.5-300		1025.1	29.7
C05-15.0-150		1035.2	31.0

References

1. Yu, W.W., (2000). “Cold-formed steel design.” John Wiley & Sons.
2. AISI. (American Iron and Steel Institute) (2013a). “Sheathing Braced Design of Wall Studs.” RP13-1, (by B.W.Schafer).
3. AISI. (American Iron and Steel Institute) (2012a). “North American Cold-Formed Steel Specification for the Design of Cold-Formed Steel Structural Members.” AISI-S100-12, Washington, DC.
4. Winter, G., (1960). “Lateral Bracing of Beams and Columns.” J. Struct. Div. 125, 809-825.
5. Winter, G., Celebi, N., and Peköz, T. (1972). “Diaphragm Braced Channel and Z-Section Beams,” Center for Cold-Formed Steel Structures Library, Paper 122.
6. AISI. (American Iron and Steel Institute) (2013b). “Rotational-Lateral Stiffness Test Method for Beam-to-Panel Assemblies.” AISI-S901-13, (revision of AISI S901-08), Washington, DC.
7. ASTM. (American Society for Testing and Materials) (2015). “Standard Test Methods of Conducting Strength Tests of Panels for Building Construction,” E72-15, ASTM International, West Conshohocken, PA, https://doi.org/10.1520/E0072-15.
8. Selvaraj, S. and Madhavan, M. (2018)."Studies on Cold-formed steel stud panels with gypsum sheathing subjected to out-of-plane bending," J. Struct. Eng.,

(ASCE), Accepted for publication. DOI : 10.1061/(ASCE)ST.1943-541X.0002069

9. Vieira Jr, L. C. M., and Schafer, B. W. (2012a). “Behavior and design of sheathed cold-formed steel stud walls under compression.” J. Struct. Eng., 139 (5) 772-786.
10. Vieira, L. C., and Schafer, B. W. (2012b). “Lateral stiffness and strength of sheathing braced cold-formed steel stud walls.” Eng. Struct., 37-205-213.
11. ASTM. (American Society for Testing and Materials) (2013). “Standard test methods for tension testing of metallic materials,” E8/E8M-13a, American Society for Testing and Materials, West Conshohocken, USA.
12. ANSI. (American National Standards Institute) (2005). “ASD / LRFD Special Design Provisions for Wind and Seismic with Commentary” ANSI/ AF&PA SDPWS-2005, Washington, DC.
13. GA. (Gypsum Association) (2010). “Gypsum board typical mechanical and physical properties.” GA-235-10, Hyattsville, MD.
14. Schafer, B.W., Vieira Jr, L.C., Sangree, R.H. and Guan, Y., (2011). “Rotational restraint and distortional buckling in cold-formed steel framing systems.” Revista Sul-americana de Engenharia Estrutural, 7(1), 71-90.
15. Papangelis, J. P., and Hancock, G. J. (1995). “Computer analysis of thin-walled structural members.” Comp. & Struct., 56(1) 157-176.
16. Li, Z., Schafer, B.W. (2010). “Buckling analysis of cold-formed steel members with general boundary conditions using CUFSM: conventional and constrained finite strip methods.” Pro. Intl. Spec. Conf. on Cold-Formed St. Struct., St. Louis, MO. November 2010.
17. AISI. (American Iron and Steel Institute) (2012b). “North American Standard for Cold-Formed Steel Framing - Wall Stud Design.” AISI S211-07, 2007 Edition (reaffirmed 2012).
18. AISI. (American Iron and Steel Institute) (2012c). “Commentary on North American Cold-Formed Steel Specification for the Design of Cold-Formed Steel Structural Members.” AISI-S100-12-Commentary, Washington, DC.
19. Wang, L., and Young, B. (2015). “Behavior of Cold-Formed Steel Built-Up Sections with Intermediate Stiffeners under Bending. II: Parametric Study and Design.” J. Struct. Eng., 142(3) 04015151.
20. ASCE. (2010). “Minimum design loads for buildings and other structures.” ASCE/SEI 7-10, ASCE, Reston, VA.
21. AS/NZS (Australian/New Zealand standard) (2002). “Structural design actions. Part 0: General principles. AS/NZS 1170.0:2002, Standards Association of Australia, Sydney, Australia.
22. Selvaraj, S. and Madhavan, M. (2018)."Studies on Cold-formed steel stud panels with gypsum sheathing subjected to out-of-plane bending," J. Struct. Eng., (ASCE), Accepted for publication. DOI : 10.1061/(ASCE)ST.1943-541X.0002069
23. Selvaraj, S. and Madhavan, M., 2019, February. Investigation on sheathing effect and failure modes of gypsum sheathed cold-formed steel wall panels subjected to bending. In Structures (Vol. 17, pp. 87-101). Elsevier.
24. Selvaraj, S. and Madhavan, M., 2019. Improvements in AISI design methods for gypsum-sheathed cold-formed steel wall panels subjected to bending. Journal of Structural Engineering, 145(2), p.04018243.
25. Selvaraj, S. and Madhavan, M., 2019, June. Sheathing bracing requirements for cold-formed steel wall panels: experimental investigation. In Structures (Vol. 19, pp. 258-276). Elsevier.
26. Selvaraj, S. and Madhavan, M., 2019. Bracing effect of sheathing in point-symmetric cold-formed steel flexural members. Journal of Constructional Steel Research, 157, pp.450-462.
27. Selvaraj, S. and Madhavan, M., 2019, August. Sheathing braced design of cold-formed steel structural members subjected to torsional buckling. In Structures (Vol. 20, pp. 489-509). Elsevier.
28. Selvaraj, S. and Madhavan, M., 2019, August. Investigation on sheathing-fastener connection failures in cold-formed steel wall panels. In Structures (Vol. 20, pp. 176-188). Elsevier.
29. Selvaraj, S. and Madhavan, M., 2019. Flexural behaviour and design of cold-formed steel wall panels sheathed with particle cement board. Journal of Constructional Steel Research, 162, p.105723.
30. Selvaraj, S. and Madhavan, M., 2019, December. Behaviour of gypsum sheathed point-symmetric cold-formed steel members: Assessment of AISI design method. In Structures (Vol. 22, pp. 76-97). Elsevier.
31. Selvaraj, S. and Madhavan, M., 2020. Structural behaviour and design of plywood sheathed cold-formed steel wall systems subjected to out of plane loading. Journal of Constructional Steel Research, 166, p.105888.
32. Selvaraj, S. and Madhavan, M., 2020. Recommendations for design of sheathing bracing systems for slender cold-formed steel structural members. Journal of Constructional Steel Research, 170, p.106116.

33. Selvaraj, S. and Madhavan, M., 2020. Influence of sheathing-fastener connection stiffness on the design strength of cold-formed steel wall panels. Journal of Structural Engineering, 146(10), p.04020202.

34. Selvaraj, S. and Madhavan, M., 2021. Criteria for selection of sheathing boards in cold-formed steel wall panels subjected to bending: construction applications and performance-based evaluation. Practice Periodical on Structural Design and Construction, 26(1), p.04020044.

35. Selvaraj, S. and Madhavan, M., 2021. Direct stiffness-strength method design for sheathed cold-formed steel structural members-Recommendations for the AISI S100. Thin-Walled Structures, 162, p.107282.

36. Selvaraj, S., Madhavan, M. and Lau, H.H., 2021, October. Sheathing-fastener connection strength-based design method for sheathed CFS point-symmetric wall frame studs. In Structures (Vol. 33, pp. 1473-1494). Elsevier.

37. Selvaraj, S., Madhavan, M. and Lau, H.H., 2021. Stiffness based design method for sheathed cold-formed steel members subjected to torsional buckling. Proceedings of the Annual Stability Conference Structural Stability Research Council 2021, SSRC 2021.

38. Selvaraj, S. and Madhavan, M., 2021. Application of Direct Stiffness-Strength Method for Design of Gypsum and Plywood sheathed CFS wall panels Subjected to Bending. Thin-Walled Structures, 180, p.109874.